

# Empirical and numerical investigation on the behaviour of foliated rock masses under high stress conditions

**E Karampinos** University of Toronto, Canada

**J Hadjigeorgiou** University of Toronto, Canada

**P Turcotte** Agnico Eagle Mines Ltd., Canada

**M-M Drolet** Agnico Eagle Mines Ltd., Canada

**F Mercier-Langevin** Agnico Eagle Mines Ltd., Canada

## Abstract

A large number of underground hard rock mines report squeezing ground conditions. The resulting deformation is often associated with the presence of foliation and high stress conditions. In order to maintain the operational integrity of excavations in squeezing ground conditions, it may be necessary to make major investments in support, and extensive rehabilitation work. This paper presents the results of field observations and numerical modelling investigations in understanding the mechanisms and parameters that control squeezing in foliated ground. A methodology for modelling such conditions using the distinct element program 3DEC is presented. The proposed technique reproduced the observed buckling mechanism and has addressed the influence of foliation and fractures within the rock mass. The results of the numerical models are reviewed with reference to the observed squeezing mechanism and deformation levels observed in the LaRonde and Lapa mines of Agnico Eagle in Canada.

## 1 Introduction

Time dependent large scale deformations in drifts have important economic implications in mining operations. In deep and high stress mines, squeezing rock conditions are generally related to the presence of prominent structural features such as a dominant fracture set, intense foliation, or a shear zone and high stress, Potvin and Hadjigeorgiou (2008). The main challenge is keeping these excavations operational and safe for workers and equipment. This requires significant rehabilitation and can result in significant support costs.

There is a limited number of documented mining case studies in squeezing ground conditions (Struthers et al. 2000; Beck & Sandy 2003; Potvin & Slade 2007; Sandy et al. 2010; Vakili et al. 2012, 2013). Useful guidelines for predicting the potential of squeezing ground conditions have been provided by Mercier-Langevin and Hadjigeorgiou (2011). Under certain conditions, the magnitude of large deformations can be reduced by choosing a favourable angle of interception between the foliation and the drift, Hadjigeorgiou et al. (2013).

Lin et al. (1984) examined failure modes of foliated rock using physical modelling. An analytical approach on eccentric loading applied in a slab under buckling loading around underground openings was examined by Kazakidis (2002). The study of the non-linear anisotropic response of foliated rock masses to stresses and excavations requires the use of numerical modelling methods. Most modelling applications in foliated rock masses have used continuum numerical methods. These techniques, however, have inherent limitations in capturing the buckling mechanism. The use of discontinuum methods although, arguably more appropriate for buckling conditions, have not seen wide use due to computational restrictions and long solution times.

Empirical and numerical investigations of squeezing conditions in foliated ground are currently in progress in two Agnico Eagle Mines Ltd. underground mines in Canada: LaRonde and Lapa. The mines provide a wide spectrum of squeezing conditions.

## 2 Theoretical criteria and empirical classifications

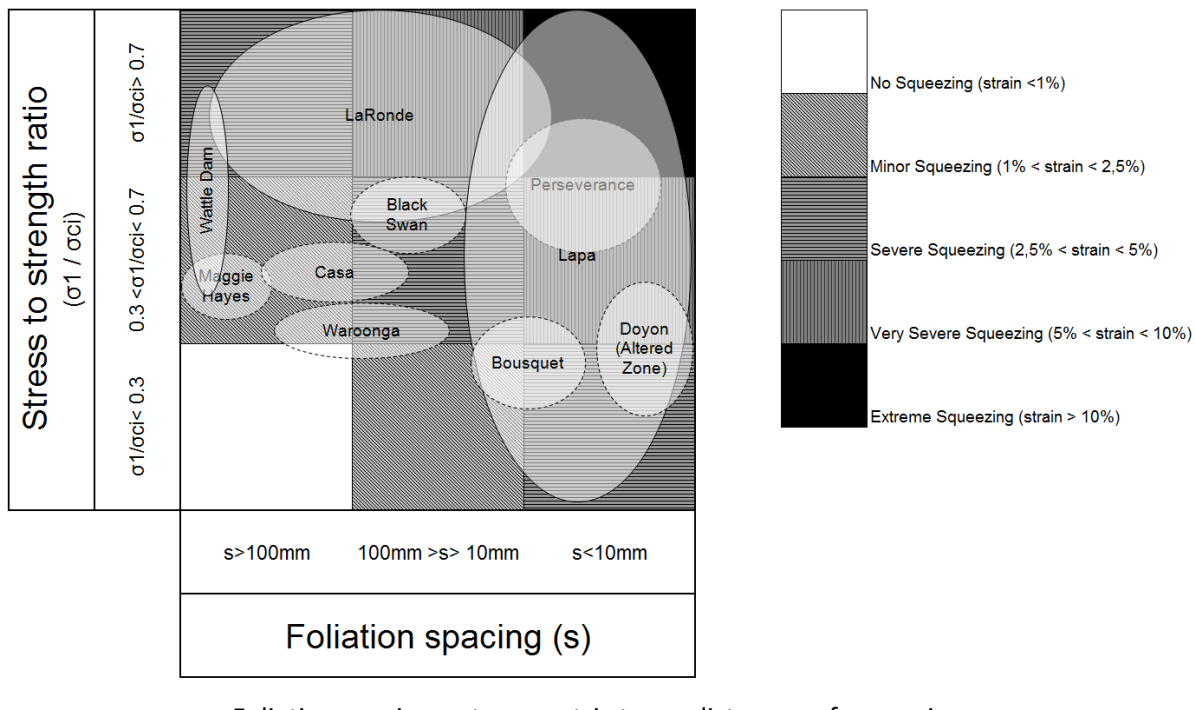
A review of theoretical criteria to quantify squeezing ground for both civil and mining applications has been provided by Potvin and Hadjigeorgiou (2008). In a mining context, Potvin and Hadjigeorgiou (2008) characterised squeezing ground conditions as closure with strain approximately greater than 2%. The host rock type in areas where squeezing was most dominant was characterised by relatively weak intact rock strength (less than 60 MPa) in addition to the presence of a prominent structure.

Mercier-Langevin and Hadjigeorgiou (2011) presented a Hard Rock Squeezing Index for underground mines based on case studies conducted in various mining operations in Australia and Canada and calibrated based on in situ observations from LaRonde Mine in Quebec, Canada. The authors noted that the index was a preliminary indicator of the squeezing potential of a rock mass and can potentially be useful in other hard rock mines experiencing squeezing ground conditions. As shown in Figure 1, the index was based on the foliation spacing of the rock mass and the stress to intact rock strength ratio. Different squeezing matrices were proposed for varying angles of interception (the angle between the normal to the plane of the wall and the normal to the foliation plane) indicating the importance of the foliation orientation in the squeezing mechanism. More severe squeezing is expected in areas with lower foliation spacing, higher stress to intact rock strength and lower angle between the orientation of the excavation and the foliation. It was also identified that the degree of squeezing increased in areas where localised alteration such as mica, chlorite and tochilinite was present.

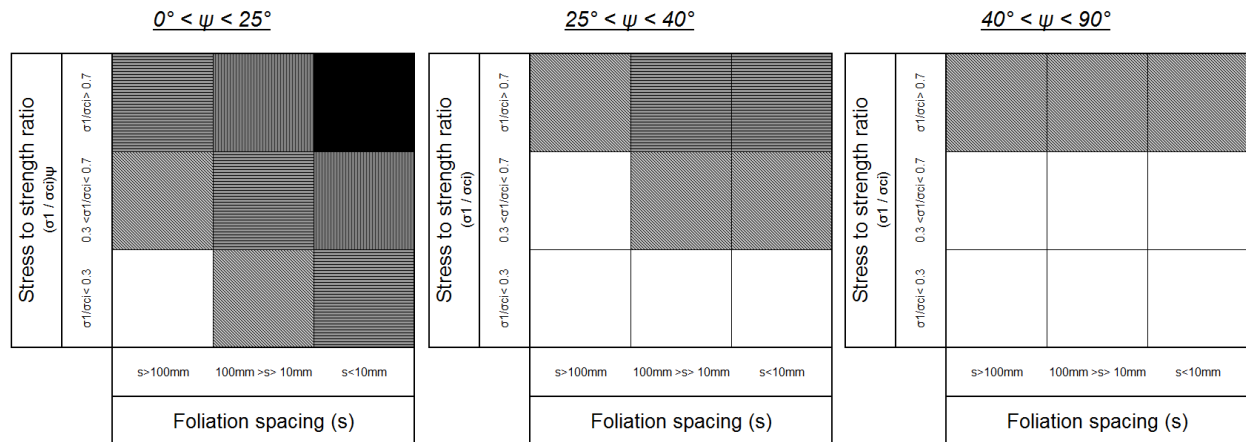
Since its introduction in 2010, the Hard Rock Squeezing Index has now been used at Wattle Dam Mine in Western Australia (Marlow & Mikula 2013) and Westwood Mine in Canada (Armatys 2012). Strain between 1 and 5% recorded in the walls of ore drives in Wattle Dam Mine matched successfully the squeezing index expectations for a range of stress to strength ratios. The squeezing areas for Wattle Dam have been included in Figure 1. Mercier-Langevin and Wilson (2013) demonstrated that the index predicted effectively the strain in a variety of conditions from no squeezing to extreme squeezing in Lapa Mine. Some cases outside the strain limits of the index with higher strain (upwards of 40%) were discussed.

The Hard Rock Squeezing Index has demonstrated the potential to be used in mining conditions. Recently, deformations outside the strain limits of the index have been recorded. Ongoing work aims to explore and extend the applicability of the Hard Rock Squeezing Index.

Hadjigeorgiou et al. (2013) updated the squeezing index database to include extreme squeezing conditions in excess of 40% strain, based on 63 case studies from LaRonde and Lapa. It is recognised that the limit of what is considered acceptable squeezing is higher in mining as opposed to tunnelling. The influence of the angle of interception between the drift and the inherent foliation was quantified further as shown in Figure 2. A higher angle of interception can result to a lower squeezing level. This was in agreement with the Hard Rock Squeezing Index (Mercier-Langevin & Hadjigeorgiou 2011) and Mercier-Langevin and Turcotte (2007) who had already reported improved conditions for haulage drifts in LaRonde driven in favourable direction with respect to the foliation. Update and extension of this database is currently in progress.



Foliation spacing – stress matrix to predict areas of squeezing



\* Where  $\psi$  is the angle between the normal to the plane of the walls of interest and the normal to the foliation planes

Squeezing matrices for varying angle of interception

**Figure 1 Squeezing ground index (modified from Mercier-Langevin & Hadjigeorgiou 2011)**

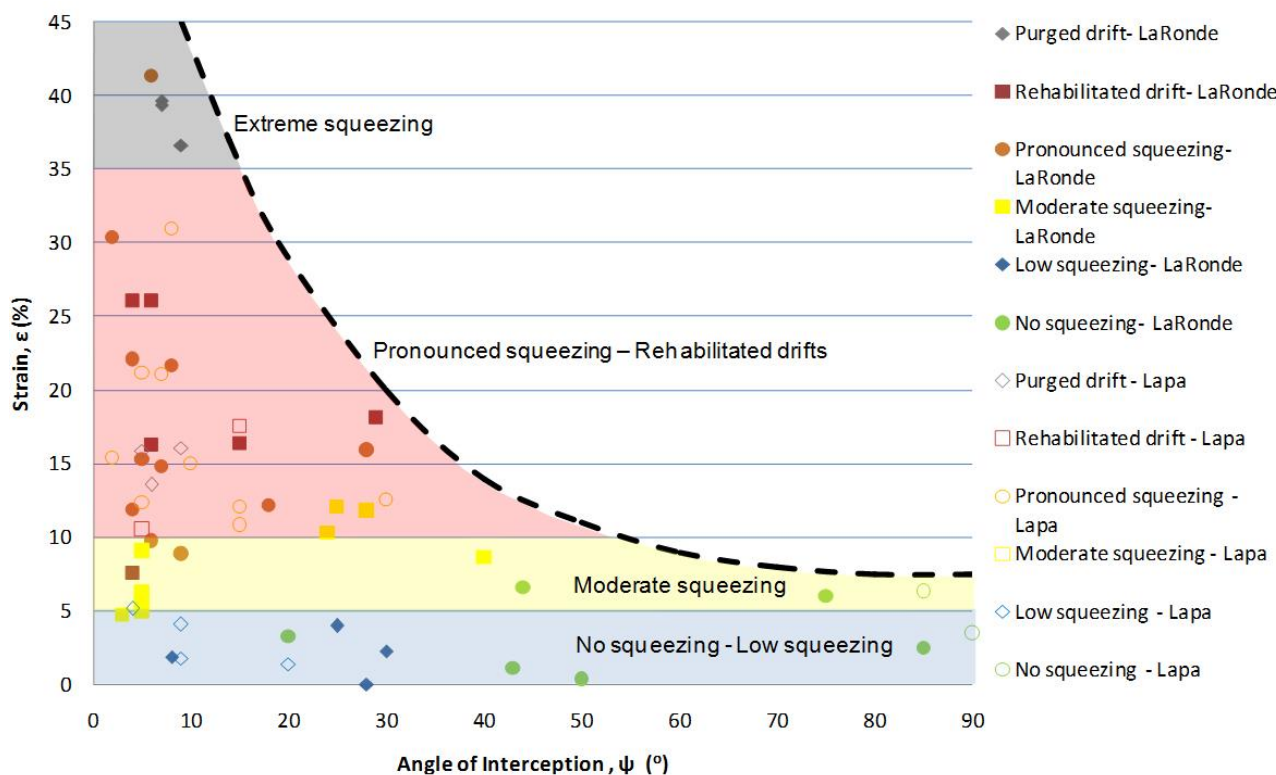


**Figure 2 Influence of angle of interception ( $\psi$ ) on resulting sidewall strain at the LaRonde and Lapa mines (Hadjigeorgiou et al. 2013)**

## 2.1 Squeezing mechanisms

Aydan et al. (1993) presented a general phenomenological description of three failure mechanisms in civil engineering tunnels related to squeezing conditions; complete shear failure of the medium; buckling failure; and shearing and sliding.

In several deep and high stress mines, including LaRonde and Lapa, squeezing rock conditions are controlled by the presence of foliation and the angle of interception between the foliation and the drift. Beck and Sandy (2003) recorded squeezing ground conditions in several Western Australian underground mines where the drives were parallel to foliation and the major principal stress was orthogonal to the excavations. Based on typical observations (Figure 3) it was suggested that bolts can be trapped and guillotined in shear. Stress induced fractures subparallel to the drive back and floor result in bulking as the fractures shear and dilate. This leads to back and floor deformation and probably drives much of the shearing in the walls. Significant bulking above the backs is initiated by the development of an open crack where the backs meet the hangingwall. Buckling of the drive walls may occur if shearing is present.

Sandy et al. (2007) noted that the support elements located at the point where the back meets the hangingwall are often the first to be sheared. When buckling occurs, it is most commonly developed in the lower part of the footwall, as a result of the confinement provided by the drive floor and the beneficial effect of reinforcement of the upper parts of the walls. The local rotation of the major principal stress around the drift, promotes the shearing in the footwall and the hangingwall.

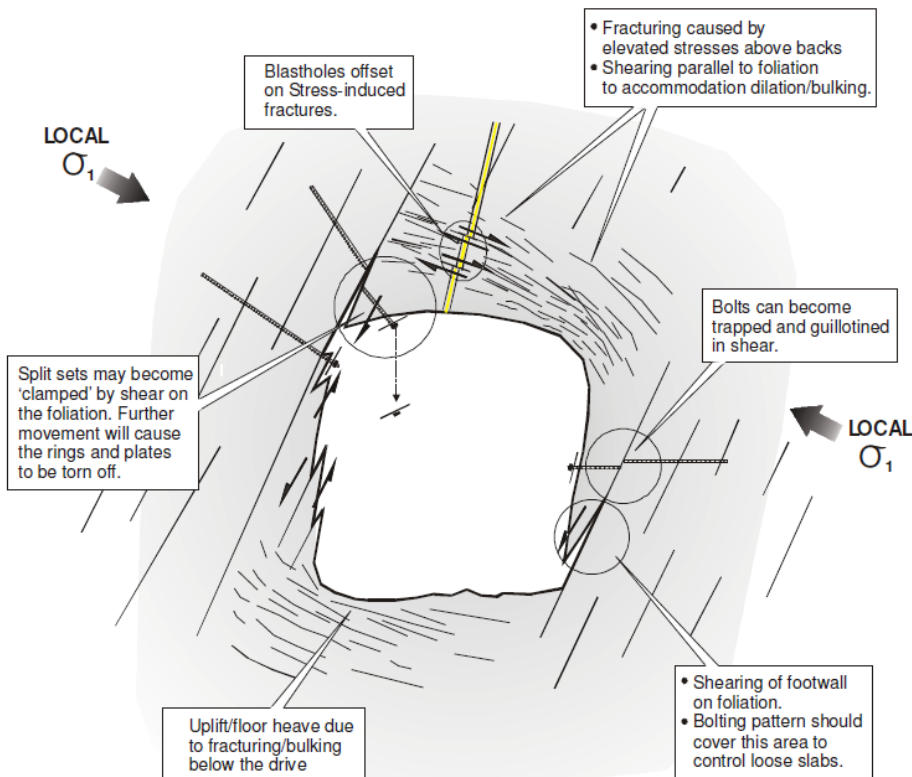


**Figure 3 Modes of large deformations ground behaviour (Beck & Sandy 2003)**

Mercier-Langevin and Wilson (2013) presented an interpretation of the failure mechanism at Lapa and the LaRonde mines. The mechanism in Figure 4 demonstrated the influence of foliation running at shallow angle to the drift. Based on their interpretation, the stress redistribution around the drift results in axial loading of foliation planes. These stresses cause the rock adjacent to the foliation to deform further. This results in contraction in the orientation of the major principal stress (along foliation) and in dilation in the direction of the minor principal stress (towards the opening). The dilation induces the deflection of the rock layers, lowering the threshold axial load necessary for buckling. As buckling takes place, this process is transferred further into the rock mass. The rock mass will bulk orthogonal to the foliation planes as more joints open up in that direction, Figure 4(b). After buckling in the walls occurs, the confinement in the floor and the back is minimal resulting to no friction between the foliation planes and a much larger relaxed zone. Early in the process the wall closure rate is high and the back and the floor are relatively stable, while later the wall closure rate decreases and the back and the floor closure rate increases.

Mercier-Langevin and Wilson (2013) also noted that deformation in competent sediments is usually minimal as opposed to weak schist. Strain in walls comprised by schist can be in excess of 40%, expressed as the ratio of deformation over the drift width. When drifts are driven at the contact of schist and sediment, squeezing conditions can be observed in only one sidewall and can extend to the back and the floor depending on which part of the drift is exposed to weak material.

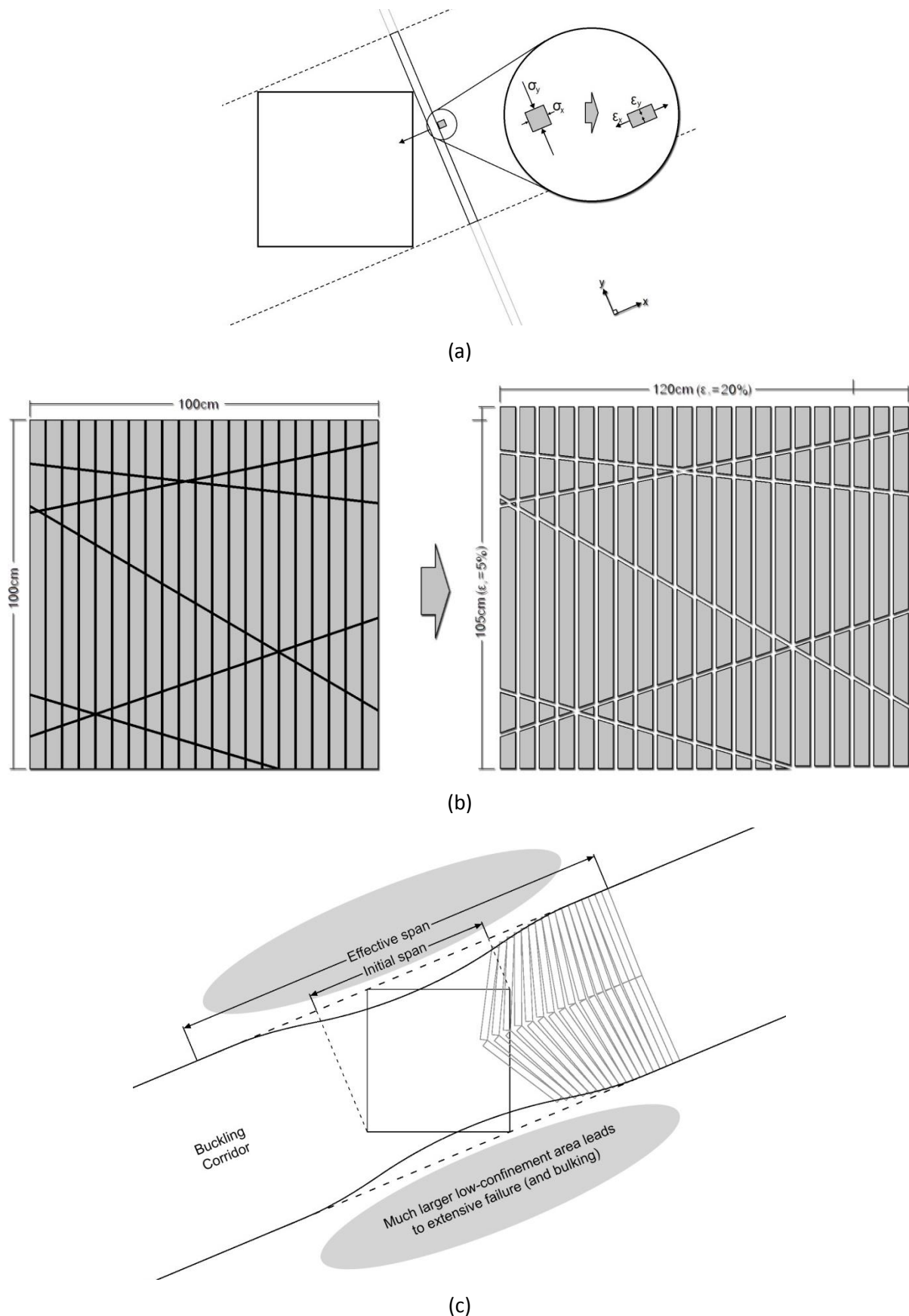


**Figure 4 Failure mechanism based on experience at Lapa and LaRonde mines; (a) initiation of buckling failure in foliated rock; (b) anisotropic rock bulking**

**following failure of foliated rock; and (c) loss of confinement on the back and floor following buckling of sidewalls (Mercier-Langevin & Wilson 2013)**

### 3 Numerical modelling applications in squeezing ground conditions

There is a plethora of documented case studies in squeezing ground conditions referring to civil engineering structures. These are not discussed further in this work. In mining applications, Sandy et al. (2007) reported that simple elastic models can predict slip on foliation but are unable to predict the location and extent of zones where stress induced fracturing occurs. In addition, they noted that an explicit representation of the foliation using the finite difference code FLAC3D (Itasca Consulting Group, Inc. 2000), successfully predicted the failure on the foliation, indicated by separation of joints. However, it did not correctly predict the location and degree of stress-induced fracturing. No reference was made on any site data so this model is regarded as a conceptual model.

Beck et al. (2010) reported some success in modelling large tunnel deformation using a multi scale approach with an explicit representation of the present structures. Each scale of model was a strain softening dilatant, discontinuum finite element model. The model included only tunnel scale or larger discontinuities, smaller scale (less than 1 m) discontinuities were homogenised. Mercier-Langevin and Turcotte (2007) used Phase<sup>2</sup> (Rocscience inc. 2005) to simulate squeezing ground conditions in LaRonde considering an elastic–plastic behaviour of the rock mass. They reported that the resulted model correlated well with the observed failure patterns. However, the model was not related to any particular drift and no deformation magnitudes were discussed. Mellies (2009) used Phase<sup>2</sup> with elastic-plastic strain softening rock mass behaviour for the representation of the failure mechanism in three drifts in LaRonde. Model calibration resulted in agreement between the measured on site and the modelled wall convergence for each drift and the models were considered as plausible solutions of the observed deformations.

A 3DEC model (Itasca Consulting Group, Inc. 2007) was used by Vakili et al. (2012) to back analyse the failure mechanism of a raise bored shaft in a highly stressed and foliated rock mass. The authors comment that the 3DEC model accurately models the observed buckling mechanism. Figure 5 shows the modelled buckling mechanism and the time dependent depth of breakout based on in situ observations. The calibrated discontinuum model was used to derive the continuum input parameters through simulated triaxial testing. A FLAC3D model was then generated using a strain softening constitutive model with ubiquitous joints which matched the associated observed damage. Vakili et al. (2013) used FLAC3D to examine the importance of the timing of support installation.

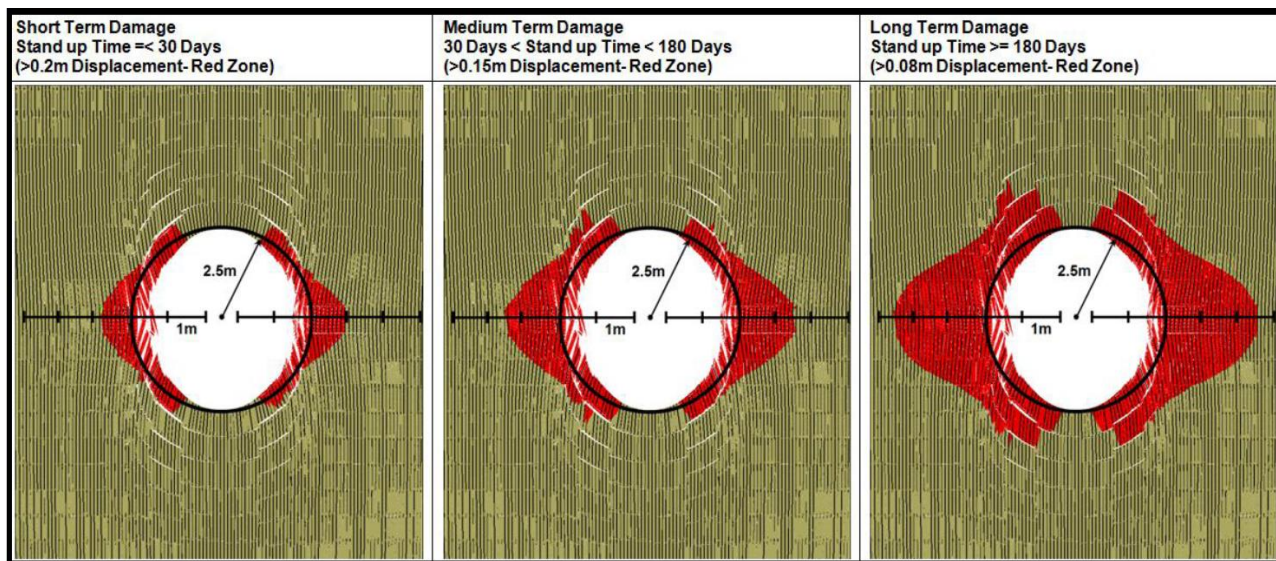


**Figure 5 3DEC modelled displacement for a raise bored shaft in highly stressed foliated rock mass (Vakili et al. 2012)**

Although numerical modelling provides a powerful tool in the analysis of squeezing ground conditions, previous work has a series of limitations. Continuum elastic-plastic numerical models such as those used by Hoek (2001) and Barla (2007) did not include the representation of any structure, and considered squeezing rock only as plastic flow of rock under the influence of high stress. Numerical modelling in squeezing ground for hard rock mines cannot be based on this assumption. Continuum modelling using the GSI for reducing the intact rock parameters has similar limitations in anisotropic conditions. Although the modelled deformation in these cases may match any observed damage, the squeezing mechanism cannot be well represented. Foliation should be modelled explicitly to allow any block rotation and buckling. Continuum modelling using finite element or finite difference methods with explicit representation of foliation can represent better the squeezing mechanism observed in hard rock mines. However, the mechanism is still not well reproduced as these methods cannot allow any block deformation or movement of blocks relative to each other. This can be achieved by using distinct element modelling. Coggan et al. (2012) provided a summary of the advantages and limitations of the most commonly used methods to analyse the rock failure around excavations discussing the ability of discontinuum discrete element methods to model the complex behaviour of rocks including block deformation and relative movement of blocks. The distinct element programs UDEC (Itasca Consulting Group, Inc. 2011) and 3DEC could better reproduce the buckling mechanism and the block detachment observed underground. However, there are no field data available to support this.

## **4 Application of the distinct element method in foliated rock mass under high stress**

Numerical modelling applications were concentrated in capturing the mechanics of the phenomenon. The 32-bit UDEC version 5.00.272 was initially used but revealed several memory limitations. Models were exceeding the maximum available memory in the program when modelling long blocks with a foliation thickness of 0.15 m. The computational restrictions were overcome by using the 64 bit three-dimensional version of the distinct element code. The 3DEC version 4.10.135 (Itasca Consulting Group, Inc. 2007) was initially used and it was later replaced by the multi-threaded 3DEC version 5.00.164 (Itasca Consulting Group, Inc. 2013).

### **4.1 Numerical modelling applications for LaRonde**

The mean foliation spacing recorded in the squeezing case studies in LaRonde varied between 0.016 m and 0.076 m. Nevertheless, a higher spacing was chosen to avoid increased running times. A conceptual model for a drift excavated parallel to the foliation at 2,270 m depth was examined (Figure 6). The foliation was dipping at 80°. The foliation thickness was 0.2 m thick near the drift and was increased to 1.2 m, 20 m away from the centre of the excavation. Horizontal joints were introduced in the model to facilitate the zoning in the blocks.

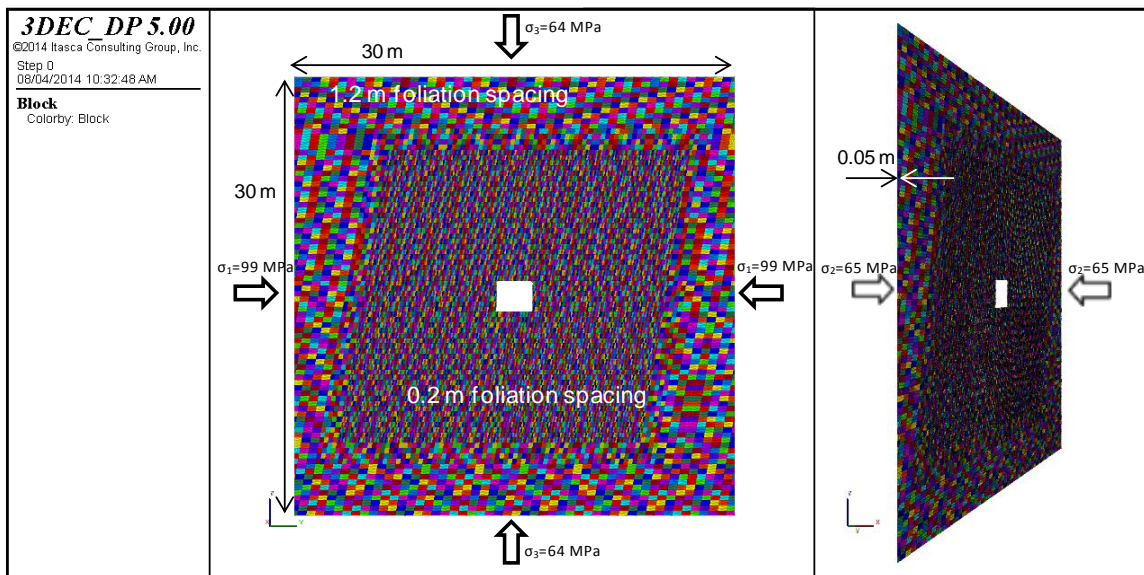


**Figure 6 Model geometry for 0.2 m foliation spacing**

The choice of constitutive block models in 3DEC was based on a series of numerical tests and iterations. The blocks created were deformable. An elastic material model was used for all discontinuities and the blocks. A Mohr–Coulomb material model was then implemented for the blocks. No residual values were used for the cohesion and the friction angle. The foliation was modelled using the ‘area contact elastic/plastic with Coulomb slip failure’ joint constitutive model (Itasca Consulting Group, Inc. 2013). An elastic material model was used for the horizontal construction joints at all times. The use of elastic material models for all joints and blocks before the application of the elastic-plastic constitutive models prevented the effect of a tensile stress wave that could cause dynamic failure in zones that would not normally fail under the static stresses caused by the excavation. The plastic zone extended to the external boundaries of the model when this modelling stage was bypassed.

The elastic mechanical properties for the intact rock (intermediate tuff) were obtained from uniaxial compressive strength tests (Turcotte 2010). A series of modelling iterations was necessary to determine the plastic properties for the intact rock and the foliation. The mechanical properties presented in Table 1 resulted to comparable squeezing levels with those recorded underground. The properties used in the numerical model were the result of a calibration process. The material properties for the intact rock and the foliation were considered to be lower than the actual in situ values. The foliation spacing used in the models is higher than the one measured underground resulting in intact rock blocks that are less prone to buckling. Reduced material properties were therefore necessary to achieve a similar level of deformation in the model with the one measured underground.

**Table 1 Material properties used in the numerical analysis**

Material properties	Input values
Young's modulus (GPa)	48
Poisson's ratio	0.16
Tensile strength of intact rock (MPa)	9
Friction angle of intact rock (°)	35°
Cohesion of intact rock (MPa)	12
Dilation angle (°)	0
Density (g/cm³)	2.81

Normal stiffness of foliation (GPa/m)	10
Shear stiffness of foliation (GPa/m)	1
Tensile strength of foliation (MPa)	0
Friction angle of foliation (°)	8
Cohesion of foliation (MPa)	0
Normal stiffness of construction joints (GPa/m)	100
Shear stiffness of construction joints (GPa/m)	10

The numerical model successfully reproduced the buckling mechanism observed underground (Figure 7). The 0.85 m displacement in the sidewalls corresponds to pronounced squeezing of 33% strain based on the classification by Hadjigeorgiou et al. (2013).

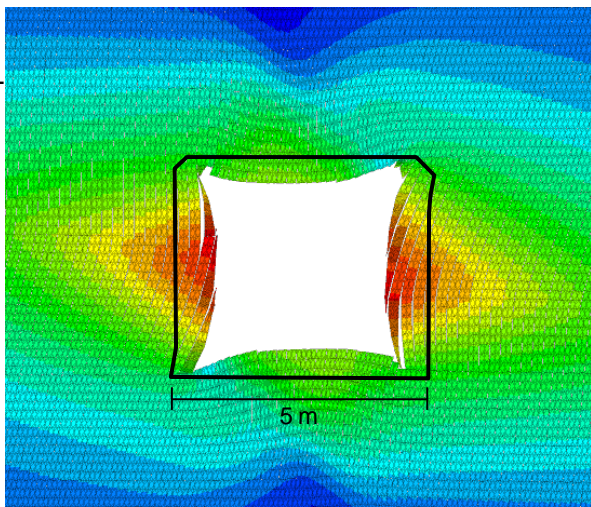
### 3DEC DP 5.00

©2014 Itasca Consulting Group, Inc.

25/03/2014 4:46:07 PM

#### Displacement magnitude

Plane: active on  
8.5000E-01 (m)  
8.0000E-01  
7.5000E-01  
7.0000E-01  
6.5000E-01  
6.0000E-01  
5.5000E-01  
5.0000E-01  
4.5000E-01  
4.0000E-01  
3.5000E-01  
3.0000E-01  
2.5000E-01  
2.0000E-01  
1.5000E-01  
1.0000E-01  
5.0000E-02  
0.0000E+00



Modelled displacement



Hangingwall at 2,550 m depth



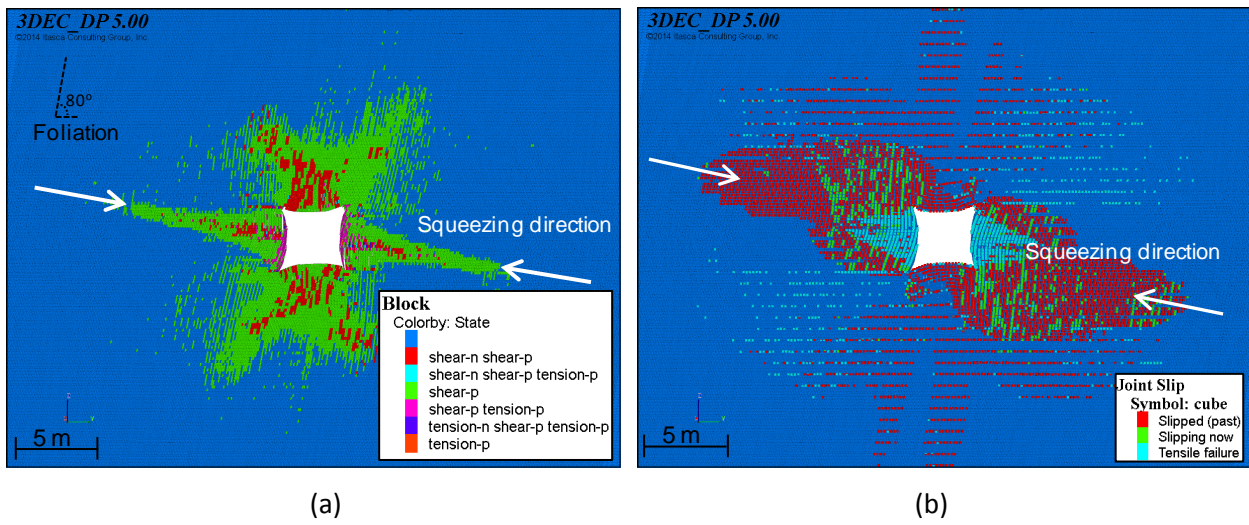
Pronounced squeezing, 2,550 m depth



Pronounced squeezing, 1,790 m depth

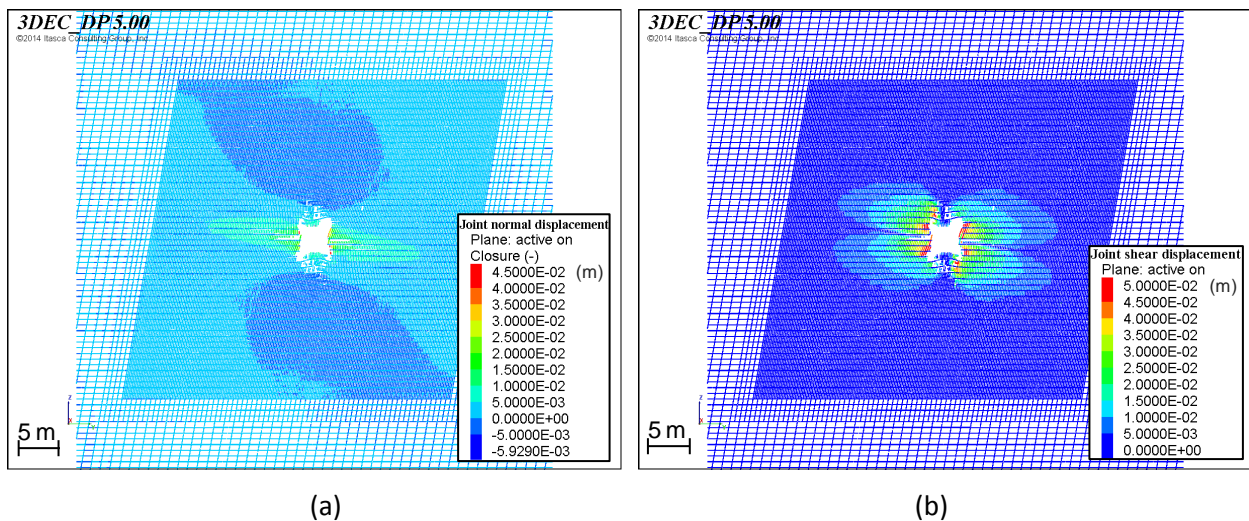
**Figure 7 Squeezing conditions in LaRonde**

Figure 8 shows the extent of the buckling area. The plastic zones around the drift show that the direction of squeezing is normal to the foliation planes. The extent of the modelled joint slip follows the direction of squeezing. The model allowed for a more refined consideration of the role of the fractures within the rock mass compared to any continuum models, resulting to block rotation, fracture opening and detachment of rock blocks from their original domain.



**Figure 8 Extent of plastic zone (a); and joint slip (b)**

Figure 9 shows the normal and shear displacement associated with the joints. The model indicates dilation in the foliation planes with a direction towards the drift. This is in agreement with the work of Mercier-Langevin and Wilson (2013). The extent of the dilation zone is comparable to the extent of the buckling zone. Closure in the foliation planes is detected in the back and the floor due to contraction above and below the drift caused by the stress redistribution after the excavation of the drift. The slipping along the joints shown in Figure 8 and the shear displacement in Figure 9 at the top of the hangingwall and the bottom of the footwall are in agreement with the shearing observed by Beck and Sandy (2003), Sandy et al. (2007) and noted in extensive field observations at LaRonde and Lapa.



**Figure 9 Joint normal displacement (a); and joint shear displacement (b)**

#### 4.2 Numerical modelling investigations for Lapa

The difference in the degree of squeezing for drifts crossing different geological units in Lapa required the introduction of more than one material in the model. A model with a strong and a weak material was generated representing the sediment and schist formation respectively. The far field stresses of level 54 (540 m deep) were assigned to the model. The maximum principal stress ( $\sigma_1$ ) was horizontal oriented north-south, the intermediate principal stress ( $\sigma_2$ ) oriented east-west and the minor principal stress ( $\sigma_3$ ) was the vertical stress. The values used were 30.2 MPa for  $\sigma_1$ , 19.5 MPa for  $\sigma_2$ , and 15.1 MPa for  $\sigma_3$ .

The foliation spacing in sediments varies between 0.01 and 0.2 m whereas in schist is usually less than 10 mm. A higher spacing of 0.075 m was used for the schist due to computational constraints and a spacing of 0.03 m was assigned to the sediments. The foliation in the models was dipping at 85° to the north. Two cases were examined; one with weak material only in the footwall of the drift; and one with the weak material extending towards the back and the floor of the drift.

The elastic properties for the intact rock were obtained from uniaxial compressive strength tests (Dubuc et al. 2011). A series of modelling iterations was necessary to determine the plastic properties for the intact rock and the foliation. The mechanical properties presented in Table 2 reproduced the displacement in the sidewall measured in level 54 for the case when there is weak material only in the footwall.

**Table 2 Material properties used in the numerical analysis**

Material properties	Input values for strong material	Input values for weak material
Young's modulus (GPa)	37.92	6.68
Poisson's ratio	0.16	0.18
Tensile strength of intact rock (MPa)	9	7
Friction angle of intact rock (°)	35	25
Cohesion of intact rock (MPa)	23.9	6.37
Dilation angle (°)	0	0
Density (g/cm <sup>3</sup> )	2.81	2.81
Normal stiffness of foliation (GPa/m)	100	10
Shear stiffness of foliation (GPa/m)	10	1
Tensile strength of foliation (MPa)	0	0
Friction angle of foliation (°)	15	8
Cohesion of foliation (MPa)	0	0
Normal stiffness of construction joints (GPa/m)	100	100
Shear stiffness of construction joints (GPa/m)	10	10

Figure 10 shows the resulting displacement obtained using the numerical model and photos from squeezing case studies at level 54 in Lapa. Although in most case studies there is actually some weak material in the back and floor, the photos are comparable to the modelling cases examined. The buckling mechanism was reproduced as in the LaRonde model. However, squeezing in these cases appeared only on the part of the drift located in the weak material. The displacement was higher for the case when the weak material was extending towards the back and the floor.

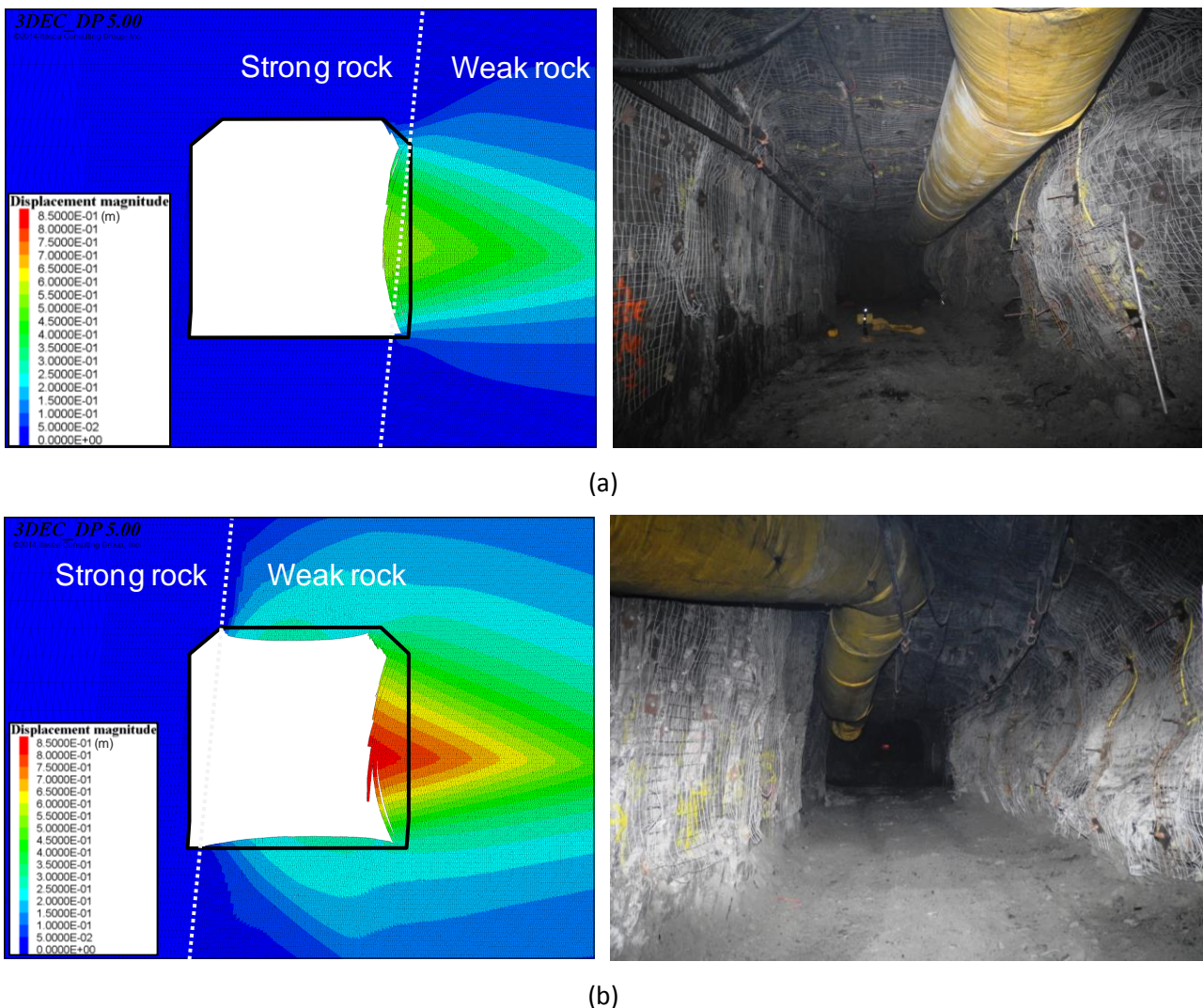


**Figure 10** Squeezing mechanisms in Lapa; weak rock in the footwall (a); and weak rock extending to back – floor (b)

#### 4.3 Numerical investigation on the foliation spacing

A parametric analysis indicated the effect of the foliation spacing on the degree of squeezing. The range of the spacing examined was between 0.05 and 0.3 m. A single material was used in this case and the in situ stresses were the same with those used in the previous model at 2,270 m depth in LaRonde. A minimum number of two zones were introduced in each block formed between the foliation. The material properties assigned to the blocks and the joints are shown in Table 3. These were higher than those used in the LaRonde model as the foliation spacing examined in this case is lower and the blocks of intact rock were more prone to buckling.

**Table 3 Material properties used for the parametric analysis**

Material properties	Input values
Young's modulus (GPa)	48.00
Poisson's ratio	0.16
Tensile strength of intact rock (MPa)	20
Friction angle of intact rock (°)	38
Cohesion of intact rock (MPa)	23
Dilation angle (°)	0
Density (g/cm <sup>3</sup> )	2.81
Normal stiffness of foliation (GPa/m)	80
Shear stiffness of foliation (GPa/m)	8
Tensile strength of foliation (MPa)	0
Friction angle of foliation (°)	8
Cohesion of foliation (MPa)	0
Normal stiffness of construction joints (GPa/m)	100
Shear stiffness of construction joints (GPa/m)	10

Figure 11 shows the resulting displacement for models with a foliation spacing of 0.3, 0.2, 0.1 and 0.05 m. There was a reduction in the displacement from 0.75 m for the 0.05 m foliation spacing model to 0.1 m for the 0.3 m foliation spacing model.

It should be clarified that the numerical models were not calibrated to specific case studies and did not include the effect of any support. Nevertheless, the resulting displacement in the models follows the same trends as described by the squeezing index and provides further confidence in its use. In addition, the numerical model methodology demonstrated the potential of 3DEC to contribute to the fine tuning, validation and extension of the squeezing index when representative models of specific case studies will be available. This will be particularly useful for investigating squeezing ground conditions under different conditions.

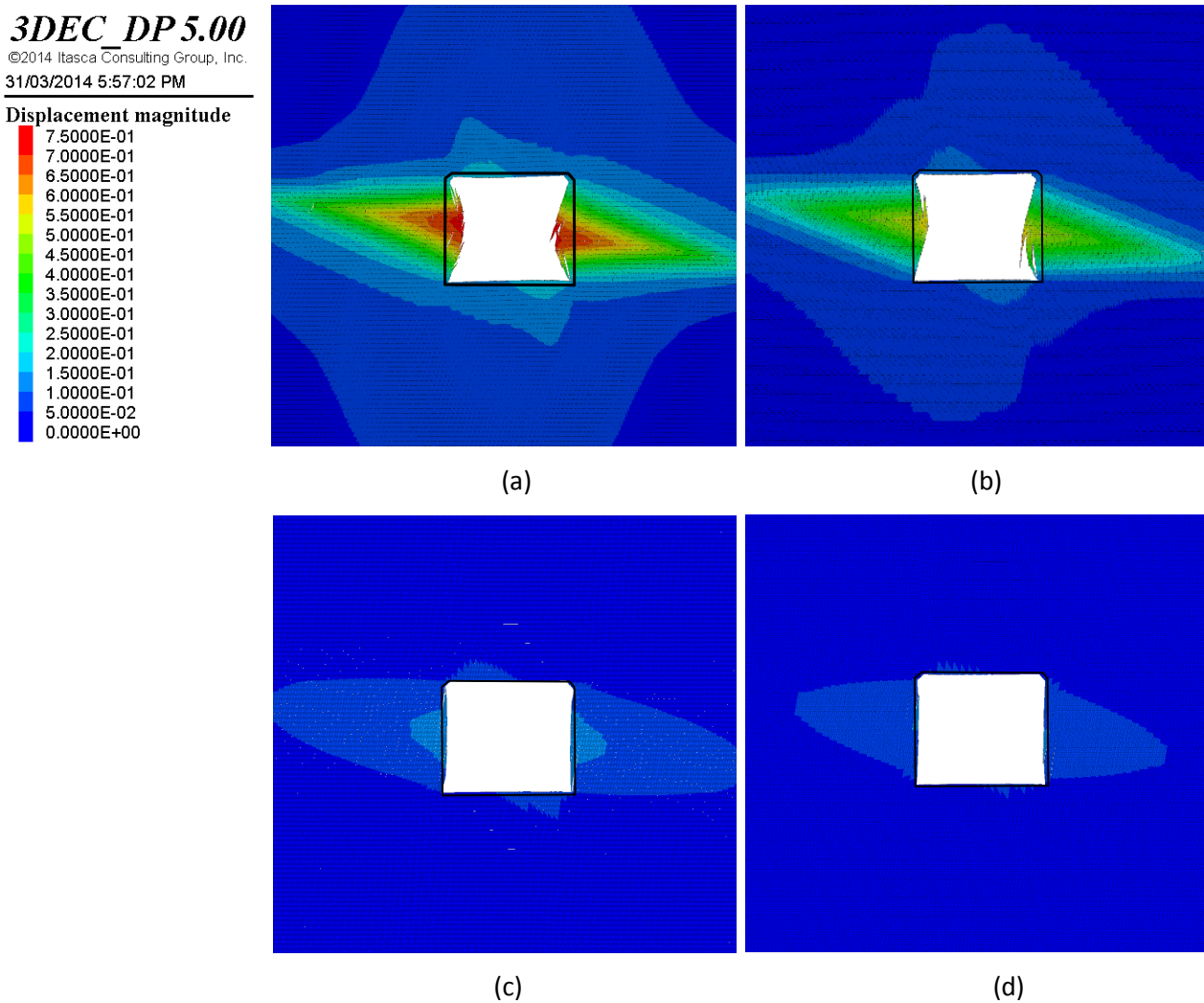


**Figure 11** Variation in the displacement for different values of foliation spacing; (a) 0.05 m spacing; (b) 0.1 m spacing; (c) 0.2 m spacing; and (d) 0.3 m spacing

## 5 Ongoing work

Further calibration of the numerical models is necessary including introducing the influence of reinforcement. Given that reinforcement is installed at different stages during the development of a drift, a 3D model is required. Modelling the advancement of a drift, using a 3D model, would not be possible due to computational and time limitations. A pseudo-3D approach can be followed instead. Current numerical applications focus on the progressive reduction of the forces at the boundaries of the excavation. This simulates the effect of reinforcement installed in different stages during the development of a drift.

## 6 Conclusions

An extension and validation process of the Hard Rock Squeezing Index (Mercier-Langevin & Hadjigeorgiou 2011) using numerical modelling and introducing more case studies is currently in progress.

The presented methodology employed a 3D distinct element model to simulate the buckling mechanism observed at the LaRonde and Lapa mines. It has been demonstrated that a better representation of the mechanism necessitates the explicit representation of foliation. The use of the distinct element method allows for a more refined consideration of the role of fractures within the rock mass. This results to modelling block rotation, fracture opening or detachment of a rock block from its original domain that would have not been possible using continuum modelling.

The constructed models represented the squeezing levels observed along drifts crossing different geological units. Modelling calibration is in an on-going progress, taking under consideration the effect of reinforcement and the 3D advancement of the drift during development.

## Acknowledgement

The authors acknowledge the support of Agnico Eagle Mines Ltd., Division LaRonde and Lapa and the Natural Sciences and Engineering Research Council of Canada. Itasca Consulting Inc. is also acknowledged for the access provided to 3DEC and UDEC and for the support offered in the use of these programs.

## References

- Armatys, M 2012, 'Modification des classifications géomécaniques pour les massifs rocheux schisteux', Masters thesis, École Polytechnique de Montréal, Montreal.
- Aydan, O, Akagi, T & Kawamoto, T 1993, 'The squeezing potential of rocks around tunnels: Theory and prediction', *Rock Mechanics and Rock Engineering*, vol. 26, no. 2, pp. 137-163.
- Barla, G, Bonini, M & Debernardi, D 2007, 'Modelling of tunnels in squeezing rock', *Proceedings of the 3rd Iranian Rock Mechanics Conference*, Iranian Society for Rock Mechanics, Tehran, pp. 1267-1285.
- Beck, DA & Sandy, MP 2003, 'Mine Sequencing for high recovery in Western Australian mines', *Proceedings of the 12th International Symposium on Mine Planning and Equipment Selection*, Australasian Institute of Mining and Metallurgy, Carlton, pp. 137-144.
- Beck, D, Kassbohm, S & Putzar, G 2010, 'Multi-scale simulation of ground support designs for extreme tunnel closure', in Y Potvin (ed.), *Proceedings of the 2nd International Symposium on block and sublevel caving*, Australian Centre for Geomechanics, Perth, pp. 441-454.
- Coggan, J, Gao, F, Stead, D & Elmo, D 2012, 'Numerical modelling of the effects of weak immediate roof lithology on coal mine roadway stability', *International Journal of Coal Geology*, vol. 90-91, pp. 100-109.
- Dubuc, R, Bédard, N, Mercier-Langevin, F, Cousin, P, Côté, J, & Archambault, M 2011, *Technical Report on the Lapa Gold Project*.
- Hadjigeorgiou, J, Karampinos, E, Turcotte, P & Mercier-Langevin, F 2013, 'Assessment of the influence of drift orientation on observed levels of squeezing in hard rock mines', in Y Potvin & B Brady (eds), *Proceedings of the Seventh International Symposium on Ground Support in Mining and Underground Construction*, Australian Centre for Geomechanics, Perth, pp. 109-118.
- Hoek, E 2001, 'Big tunnels in bad rock', *ASCE Journal of Geotechnical and Geoenvironmental Engineering*, vol. 127, no. 9, pp. 726-740.
- Itasca Consulting Group, Inc. 2000, 'FLAC3D: Fast Analysis of Continua in 3 Dimensions', Itasca Consulting Group, Inc., Minneapolis, <http://www.itascacg.com/software/flac3d>
- Itasca Consulting Group, Inc. 2007, '3DEC: Three-Dimensional Distinct Element Code', version 4.10.135, Itasca Consulting Group, Inc., Minneapolis, <http://www.itascacg.com/software/3dec>
- Itasca Consulting Group, Inc. 2011, 'UDEC: Universal Distinct Element Code', Itasca Consulting Group, Inc., Minneapolis, <http://www.itascacg.com/software/udec>
- Itasca Consulting Group, Inc. 2013, '3DEC: Three-Dimensional Distinct Element Code', version 5.00.164, Itasca Consulting Group, Inc., Minneapolis, <http://www.itascacg.com/software/3dec>
- Kazakidis, VN 2002, 'Confinement effects and energy balance analyses for buckling failure under eccentric loading conditions', *Rock Mechanics and Rock Engineering*, vol. 35, no. 2, pp. 115-126.
- Lin, Y, Hong, Y, Zheng, S & Zhang, Y 1984, 'Failure modes of openings in a steeply bedded rock mass', *Rock Mechanics and Rock Engineering*, 17, vol. 113-119.
- Marlow, P & Mikula, PA 2013, 'Shotcrete ribs and cemented rock fill ground control methods for stoping in weak squeezing rock at Wattle Dam Gold Mine', in Y Potvin & B Brady (eds), *Proceedings of the Seventh International Symposium on Ground Support in Mining and Underground Construction*, Australian Centre for Geomechanics, Perth, pp. 133-148.
- Mellies, G 2009, 'Two case studies of excavations in fractured rock', MSc thesis, Université Laval, Quebec.
- Mercier-Langevin, F & Turcotte, P 2007, 'Expansion at depth at Agnico Eagle's LaRonde Division – meeting geotechnical challenges without compromising production objectives', in Y Potvin, J Hadjigeorgiou & D Stacey (eds), *Challenges in Deep and High Stress Mining*, Perth, Australian Centre for Geomechanics, pp. 189-195.
- Mercier-Langevin, F & Hadjigeorgiou, J 2011, 'Towards a better understanding of squeezing potential in hard rock mines', *Transactions of the Institution of Mining and Metallurgy, Section A: Mining Technology*, vol. 120, no. 1, pp. 36-44.
- Mercier-Langevin, F & Wilson, D 2013, 'Lapa mine – ground control practices in extreme squeezing ground', Y Potvin & B Brady (eds), *Proceedings of the Seventh International Symposium on Ground Support in Mining and Underground Construction*, Australian Centre for Geomechanics, Perth, pp. 119-132.
- Potvin, Y & Slade, N 2007, 'Controlling extreme ground deformation – learning from four Australian case studies', in Y Potvin, J Hadjigeorgiou & D Stacey (eds), *Challenges in Deep and High Stress Mining*, Perth, Australian Centre for Geomechanics, pp. 355-361.
- Potvin, Y & Hadjigeorgiou, J 2008, 'Ground support strategies to control large deformations in mining excavations', *Journal of the South African Institute of Mining and Metallurgy*, vol. 108, no. 7, pp. 393-400.

- Rocscience inc. 2005, 'Phase<sup>2</sup>: Finite Element Analysis for Excavations and Slopes', Rocscience inc., Toronto, <https://www.rocscience.com/products/3/Phase2>
- Sandy, MP, Gibson, W & Gaudreau, D 2007, 'Canadian and Australian ground support practices in high deformation environments', in Y Potvin (ed.), *Proceedings of the Fourth International Seminar on Deep and High Stress Mining*, Perth, Australian Centre for Geomechanics, pp. 297-311.
- Sandy, MP, Sharrock, G & Vakili, A 2010, 'Managing the Transition from Low Stress to High Stress Conditions', in PC Hagan & S Saydam (eds), *Proceedings of the Second Australasian Ground Control In Mining Conference*, Australasian Institute of Mining and Metallurgy, Carlton, on CD-ROM.
- Struthers, MA, Turner, MH, McNabb, K & Jenkins, PA 2000, 'Rock mechanics design and practice for squeezing ground and high stress conditions at Perseverance mine', in G Chitombo (ed.), *Proceedings MassMin 2000*, Australasian Institute of Mining and Metallurgy, Carlton, pp. 755-764.
- Turcotte, P 2010, 'Field behaviour of hybrid bolt at LaRonde Mine', in M Van Sint Jan & Y Potvin (eds), *Proceedings of the Fifth International Seminar on Deep and High Stress Mining*, Australian Centre for Geomechanics, Perth, pp. 309-319.
- Vakili, A, Sandy, MP & Albrecht, J 2012, 'Interpretation of non-linear numerical models in geomechanics – a case study in the application of numerical modelling for raise bored shaft design in a highly stressed and foliated rock mass', *Proceedings of the 6th International Conference and Exhibition on Mass Mining: MassMin 2012*, Canadian Institute of Mining, Metallurgy and Petroleum, Westmount, on CD-ROM.
- Vakili, A, Sandy, MP, Mathews, M & Rodda, B 2013, 'Ground support design under high stressed conditions', in Y Potvin & B Brady (eds), *Proceedings of the Seventh International Symposium on Ground Support in Mining and Underground Construction*, Australian Centre for Geomechanics, Perth, pp. 551-564.

